



AUTHOR(S):

TITLE:

YEAR:

Publisher citation:

OpenAIR citation:

Publisher copyright statement:


This is the _____ version of an article originally published by _____
in _____
(ISSN _____; eISSN _____).

OpenAIR takedown statement:

Section 6 of the "Repository policy for OpenAIR @ RGU" (available from <http://www.rgu.ac.uk/staff-and-current-students/library/library-policies/repository-policies>) provides guidance on the criteria under which RGU will consider withdrawing material from OpenAIR. If you believe that this item is subject to any of these criteria, or for any other reason should not be held on OpenAIR, then please contact openair-help@rgu.ac.uk with the details of the item and the nature of your complaint.

This publication is distributed under a CC _____ license.

The parameter identification method study of the splice equivalent circuit model for the aerial lithium-ion battery pack

Measurement and Control
2018, Vol. 51(5-6) 125–137
© The Author(s) 2018
Reprints and permissions:
sagepub.co.uk/journalsPermissions.nav
DOI: 10.1177/0020294018770930
journals.sagepub.com/home/mac


Shunli Wang¹ , Carlos Fernandez², Xiaohan Liu¹, Jie Su¹
and Yanxin Xie¹

Abstract

According to the special condition expression of the aerial lithium-ion battery pack, a novel targeted equivalent model (Splice–Equivalent Circuit Model) is proposed and constructed. The Splice–Equivalent Circuit Model achieves the accurate mathematical expression of the special operating conditions and the working process for the lithium-ion battery pack, which is realized by using the equivalent simulation of different internal effects in the charging and discharging process of the battery pack. The theoretical study and analysis of the working principle is investigated to express the working characteristics of the aerial lithium-ion battery pack together with the experimental analysis. Then, the equivalent circuit model of the aerial lithium-ion battery pack is carried out on the composite construction methods. The experimental studies are carried out in order to identify the parameters of the improved Splice–Equivalent Circuit Model, obtaining respectable identification results of battery equivalent model parameters.

Keywords

Aerial lithium-ion battery pack, splice equivalent circuit model, working characteristics, partial least square, output voltage tracking

Date received: 9 September 2017; accepted: 11 February 2018

Introduction

The equivalent model is often used to simulate the dynamic characteristics of the lithium-ion battery. However, a simple model cannot reflect the dynamic changes of the battery, which may lead to the incorrect recognition results. Meanwhile, the complex model needs to determine too many parameters and the computational complexity will increase greatly, which may bring in the divergence of parameters. The aerial lithium-ion battery pack is cascaded by many battery cells to achieve the high power applications and the large capacity requirements for the required energies. The equivalent model construction methods are explored for the accurate working characteristic expression of the lithium-ion batteries. Because the external characteristics can describe the importance of the batteries, the equivalent circuit modeling method is employed by using the experimental data, in which the chemical reaction is considered without the applicability of the battery.

Beattie et al.¹ investigated the capacity fade in silicon-based electrodes for lithium-ion batteries using three electrode cells and upper cut-off voltage. Bauer et al.² reported

the dilation relaxation behavior of graphite-based lithium-ion battery cells. Wang et al.³ proposed an integrated online adaptive state of charge (SOC) estimation approach of high power lithium-ion battery packs. Cacciato et al.⁴ built a real-time model-based state estimation (SOC) for energy storage systems. Chen et al.⁵ constructed a multi-winding transformer cell-to-cell active equalization method for lithium-ion batteries with reduced number of driving circuits. Chen et al.⁶ proposed a robust adaptive sliding-mode observer using the neural network for the SOC estimation

¹School of Information Engineering and Robot Technology Used for Special Environment Key Laboratory of Sichuan Province, Southwest University of Science and Technology, Mianyang, China

²School of Pharmacy and Life Sciences, Robert Gordon University, Aberdeen, UK

Corresponding author:

Shunli Wang, School of Information Engineering and Robot Technology Used for Special Environment Key Laboratory of Sichuan Province, Southwest University of Science and Technology, Mianyang 621010, China
Email: wangshunli@swust.edu.cn



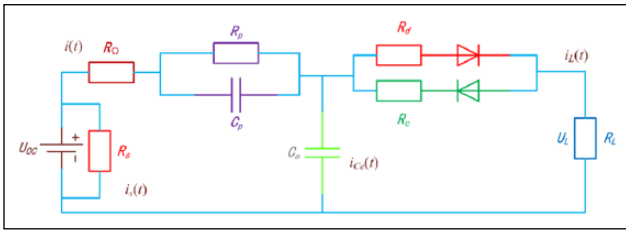


Figure 1. The improved equivalent circuit model of S-ECM.

of the lithium-ion battery. Bresciana et al.⁷ proposed a combined investigation on local permanent degradation in a direct methanol fuel cell. Abadaa et al.⁸ proposed a safety modeling method of lithium-ion batteries. The average cycling current effect on the total energy of the lithium-ion battery is studied by Barai et al.⁹ Dubarry et al.¹⁰ detect the cell-balancing currents. Hu et al.¹¹ summarize the technological developments in batteries. A reduced low-temperature electro-thermal coupled model is constructed by Jiang et al.¹² Koca et al.¹³ study the energy flow control strategies. A simplified multi-particle model is constructed by Li et al.¹⁴ The fading KF-based real-time SOC estimation is conducted by Lim et al.¹⁵ Liu et al.¹⁶ propose a new method of modeling and SOC estimation. Liu et al.¹⁷ did the energy management with automated mechanical transmission. Martel et al.¹⁸ conduct the long-term assessment for the battery lifetime degradation management. Ozer et al.¹⁹ conduct the energy flow control. Sarasketa-Zabala et al.²⁰ propose a realistic lifetime prediction approach. Saw et al.²¹ describe the integration issues of the battery pack. Soylu and Bayir²² conduct the measurement of electrical conditions. Sung et al.²³ did the robust and efficient capacity estimation using data-driven meta model. The electrochemical battery model and its parameter estimator are constructed by Sung et al.²⁴ The online dynamic equalization adjustment is conducted by Wang et al.²⁵ A novel safety anticipation estimation method is proposed by Wang et al.²⁶ An adaptive remaining energy prediction approach is proposed by Wang et al.²⁷ The enhanced online model identification is conducted by Wei et al.²⁸ The parameter sensitivity is analyzed by Zhou et al.²⁹ for fractional-order modeling. Experimental investigation on an integrated thermal management system has been studied by Zou et al.³⁰ As can be seen from the above reference analysis, the equivalent circuit model is quite necessary for the working state monitoring and energy management of the lithium-ion battery packs in the power supply application.

In order to adapt the challenging working environment of the aerial safety auxiliary power application, the construction method of the equivalent circuit model is investigated first based on the single consistent assumption through all the lithium-ion battery cells. The lithium-ion battery will be equivalent to a single battery cell with higher voltage and larger capacity. At the same time, the cell consistency parameter is introduced and considered for the group working conditions of the internal connected lithium-ion battery cells by using the proposed equivalent model construction method. Then, different equivalent

simulation methods are conducted through the exploratory application and analyzed by the equivalent modeling. Meanwhile, the analysis and application are targeted to improve exploration on various equivalent models, combined with the improvement ideas by analyzing the advantages and disadvantages of various existing methods. Finally, a specific battery equivalent model is proposed and used for the aerial lithium-ion battery pack to meet the requirements of its safe application and avoid the security accident.

Mathematical analysis

The Splice–Equivalent Circuit Model construction method study

According to the special working condition and working state description target of the aerial lithium-ion battery pack, the composite equivalent circuit model (Splice–Equivalent Circuit Model (S-ECM)) is put forward considering the characterization accuracy and the computational complexity by using the improved equivalent circuit method, combined with the advantage analysis of the empirical equation model, one-order RC, PNGV and Thevenin. The S-ECM model is constructed by considering the different effects of the internal aerial lithium-ion battery cells on the cascaded group. In order to achieve the accurate mathematical special working condition description of the aerial lithium-ion battery pack in the working process, the shunt resistance employs the one-order RC which is based on the equivalent characterization of the self-discharge effect as well as describing the working process of the lithium-ion battery pack accurately. According to the application conditions and characteristics of the aerial lithium-ion battery, the characteristics of the original battery equivalent model combined with the equivalent circuit mode theory are analyzed in order to improve the working characteristics of the expression effect. The structure of the improved equivalent circuit model S-ECM is shown in Figure 1.

The symbols in Figure 1 are described as follows. The parameter U_{oc} is used as the Open Circuit Voltage (OCV) of the battery characterization of the aerial lithium-ion battery pack. R_s is the high resistance for self-discharge effect characterization of the lithium-ion battery pack. The parameter R_{Ω} represents the battery ohm resistance, in which the voltage drop characterization of the lithium-ion battery during the charge and discharge process of positive and negative across the S-ECM can be realized. The proposed model can be obtained by using the one-order RC parallel circuit. The purpose is to simulate the relaxation effect characterization in the charge and discharge maintenance process and the battery transient response expression. The polarization resistance R_p characterizes the polarization effect of the lithium-ion battery pack together with the polarization capacitance parameter C_p . In addition, the parallel circuit parameters reflect the polarization effect of lithium-ion battery pack on production and elimination. R_d is the discharge resistance that characterizes the resistance difference in the discharge

period. R_c is the charging resistance for the resistance difference characterization in the charging process of the aerial lithium-ion battery pack. The capacitance parameter C_e is used to describe the surface effect of lithium-ion battery pack. $U_L(t)$ is the voltage value of the battery pack that is connected with the external circuit. This is also the terminal voltage of the positive and negative ends for the aerial lithium-ion battery pack in the charge and discharge working process with the current $I_L(t)$ inflow or outflow of the aerial lithium-ion battery pack. The current parameter $I_L(t)$ is set to be positive in the discharge process and negative in the charging process.

State space mathematical description

The state space equation of the equivalent model S-ECM has been constructed for the special working condition of the aerial lithium-ion battery pack, which is the equivalent modeling of the internal state for the battery pack. Considering the mathematical representation of the known experimental data analysis application, the parameter coefficient estimation results can realize the effective modeling of the lithium-ion battery pack. Therefore, it is invaluable to achieve an equivalent state space model representation and construct the SOC estimation model foundation of the aerial lithium-ion battery pack.

The proposed S-ECM model has the following components to characterize the working state accurately for the aerial lithium-ion battery pack. The ideal voltage source equivalent parameter U_{oc} describes the OCV of the lithium-ion battery pack. Meanwhile, the high megohm resistor R_s denotes the self-discharge effect for the aerial lithium-ion battery pack characterization. The milliohm level small R_Ω is the ohmic resistance for the resistor characterization. The characterization parameters of R_p and C_p symbolize the polarization resistance and capacitance, respectively. The parallel circuit reflects the generation process and the cell polarization elimination. U_L is used for the terminal voltage characterization when connected with the external circuit. R_d signifies the discharge resistance, which is used to characterize the resistance difference in the discharging process. Meanwhile, R_c is the charging resistance, which is used to characterize the resistance difference in the charging process. The discharge current provisions can be obtained in the forward direction, which can repress the working SOC and discharge for the aerial lithium-ion battery pack. The characterization of relationship between each terminal voltage between the circuit components can be described according to the model and Kirchhoff's law, in which the state space equation can be described as shown in equation (1)

$$\begin{cases} R_\Omega * \left(\frac{U_p}{R_p} + C_p \frac{dU_p}{dt} \right) + U_p + I(t)R_{cd}(t) = U_{OC} - U_L \\ I_e(t) = C_e \frac{dU_e}{dt} = \left| C_p \frac{dU_p}{dt} + \frac{U_p}{R_p} - I(t) \right|; I_s(t) = \frac{U_{OC}}{R_s} \end{cases} \quad (1)$$

Aiming to simplify the describing process of the state space equations, $R_{cd}(t)$ is utilized for the resistance difference characterization in the charge and discharge process instead of using the difference resistance parameters of R_c and R_d . When the aerial lithium-ion battery pack is in the discharge process, $R_{cd}(t)$ is set to $R_{cd}(t)=R_d$. Meanwhile, when the aerial lithium-ion battery pack is in the charging process, the parameter value is set as $R_{cd}(t)=R_c$. The capacitance parameter C_e is employed for the surface effect characterization of the aerial lithium-ion battery pack. According to the structure analysis of the S-ECM circuit, the accurate description of its state space can be carried out. The voltage drop on the capacitor parameter C_e can be described by using the voltage parameter U_e , and U_{OC} is the OCV. When the lithium-ion battery pack is in the open circuit state, the relation between these voltage parameters can be described by the equation $U_{OC}=U_e=U_L$. According to the acquisition target of the observation equation and the analysis of the equivalent circuit model, the upper model is analyzed and transformed, in which the state space equation expression of the transformation can be obtained as shown in equation (2)

$$U_L = U_{OC} - R_\Omega * \left(\frac{U_{Cp}}{R_p} + C_p \frac{dU_{Cp}}{dt} \right) + U_{Cp} + I(t)R_{cd}(t) \quad (2)$$

The basic equation framework of the estimation process can be established by using the state space model in the charge and discharge process, combining the identification process of the model parameters, which can be used for the subsequent SOC estimation research. Thus, the model parameter identification system can be designed by the determination of the state space equation, in which the parameter identification of the S-ECM model is a dynamic system. In the system parameter identification process, the modular design for the parameter identification is a simple and direct solution. This method is very suitable for the dynamic system identification of model parameters and it has strong adaptability to realize the time domain estimation of dynamic parameters. This is implemented by using the dynamic principle of the parameter identification module. Therefore, the corresponding output values of the model parameters can be identified effectively.

The discrete mathematics variation detection and model parameters of discrete time are necessary in the system stabilization and parameter identification process, in which the dynamic state space equation and expression can be realized by the mathematical characteristics. When using the identification process of the network, the energy equation of the identification error function is defined by the equivalent standard, and the function can be achieved through the dynamic equation and the parameter identification module, which can obtain the accurate identification results. The equivalent model and the state space equation, combined with the SOC estimation demand, are the important parts for the aerial lithium-ion battery pack. This

Table 1. The basic parameters of the experimental samples.

ID	Parameter name	Symbols	Experimental requirements
[01]	Open circuit voltage	U_{oc}	Full charge, intermittent discharge and shelving measurements
[02]	Self-discharge resistance	R_s	Current open circuit voltage is measured with open circuit voltage after 30 days
[03]	Ohmic resistance	R_Ω	HPPC test in intermittent discharge
[04]	Polarization resistance	R_p	Experimental process, requirement, ohmic resistance
[05]	Polarization capacitance	C_p	Experimental process, requirement, ohmic resistance
[06]	The differential internal resistance of discharge	R_d	The pulse discharge process in HPPC test is combined with ohmic internal resistance
[07]	Charging differential resistance	R_c	It is obtained in the pulse charging process of HPPC test, combined with ohmic internal resistance
[08]	The surface effect capacitance	C_e	Measured at open circuit voltages of 0% and 100% at SOC, respectively

HPPC: Hybrid Power Pulse Characterization; SOC: state of charge.

includes the parameters of the terminal voltage, single cell voltage, current and temperature as well as conducting the state equation of the model parameter identification system. As the data acquisition and processing steps are discrete in the actual calculation process, the dispersing process of the state space description can be conducted as shown in equation (3)

$$\begin{cases} U_L(k) = U_{OC}(k) - R_\Omega * I(k) - U_p(k) - I(k)R_{cd}(k) \\ U_p(k+1) = U_p(k)e^{-\Delta t/\tau} + I(k)R_p(1 - e^{-\Delta t/\tau}) \end{cases} \quad (3)$$

The physical meanings of the symbols in the above equation are described as follows. k represents the parameter detection time point. $U_L(k)$ describes the terminal voltage at the k time point. R_Ω denotes the ohmic resistance, and $I(k)$ is the output current. $U_p(k)$ symbolizes the voltage characterization at both ends of the circuit parameters for the polarization resistance and capacitance. The detection cycle time parameter τ is used for the time constant of the RC parallel circuit. R_p is employed as the polarization resistance in the equivalent circuit model, which can be characterized by the parameters of $U_p(k+1)$ and $U_p(k)$, respectively, characterizing the voltage polarization resistance values for the $k+1$ and k time points at the both ends of the RC circuit.

Parameter identification experiments

The target acquisition parameters of the S-ECM model can be obtained by carrying out a variety of charge and discharge pulse combination experiments. The real-time detection of the output voltage can be conducted corresponding to the response, and then the model coefficient change law of the equivalent model can be obtained for the working state characterization through the experimental and calculation principle analysis. The equivalent model analysis can be realized in SIMULINK, in which the change of each factor in the model and its overall working state are analyzed. The identification parameters are set in the S-ECM model of the lithium-ion battery pack and the experimental requirements can be obtained by combining

the model analysis in the model parameter identification process, which are shown in Table 1.

In view of the experimental requirements listed above, the intermittent discharge and charge experiments (Hybrid Power Pulse Characterization (HPPC)) are carried out to obtain the parameters of each model parameter and its changing law. This aims to obtain the required output voltage changes in response to the charging and discharging process. The SOC value reaches 100% by the periodical constant current and voltage (Constant Current–Constant Voltage (CC-CV)) charging maintenance process, making it to be full of electricity. Thus, it is set to be quiescence for half an hour to make its internal electrochemical reaction to be stable. Afterward, the following test expand can be conducted. The 0.2C₅A current intermittent discharge step was carried out in the experimental process, and the HPPC experiment was carried out at the end time point of the shelving state period for 30 min. The discharge process of constant discharge suspends for 30 min in the process of HPPC test, and the HPPC hybrid pulse test can be turned aside after 30 min of incubation. Meanwhile, the closed circuit voltage and current changes are recorded in the experimental test process. After the test is completed, the constant current discharge and the experimental test are continued according to the above process until the SOC is discharged to be 0.00%. The cyclic process is described as shown in Figure 2.

As can be known from Figure 2, the hollow circle symbolizes the HPPC test embedded in the intermittent discharge process. The current is expanded in each batch by using the last sustained 5.00 s pulses at the end time point. Aiming at the parameter identification goal of the S-ECM model, the state space equations are utilized for the working state characterization of the aerial lithium-ion battery pack. The experiments are conducted at room temperature of 25.00 °C, in which the mixed HPPC pulse test together with the 1C₅A constant current pulse charge and discharge test are conducted by using the power characteristics. The model parameters for the SOC correlation treatment are obtained through the pulse charging and discharging process, combining with the working principle analysis of the aerial lithium-ion battery pack. As can be known from the experimental analysis, the dynamic characteristics of the

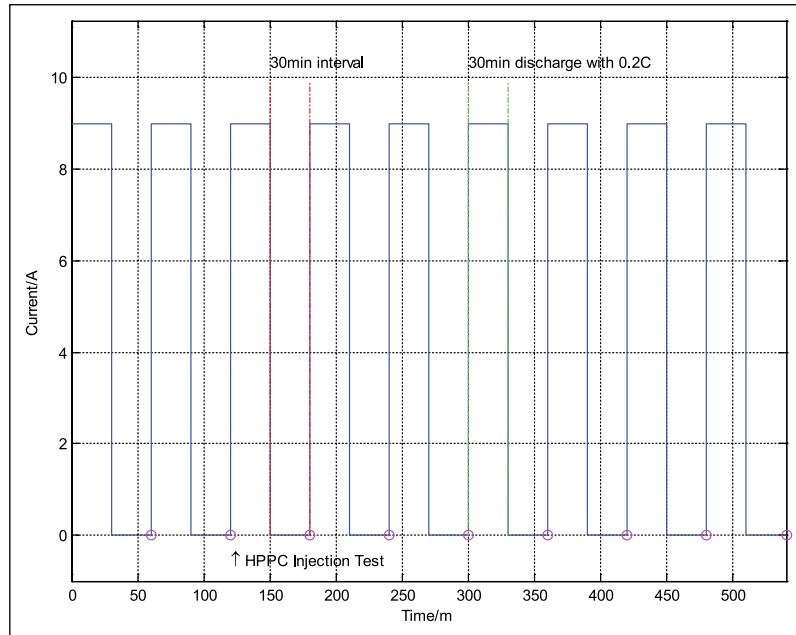


Figure 2. The pulse charging-discharging experiment.

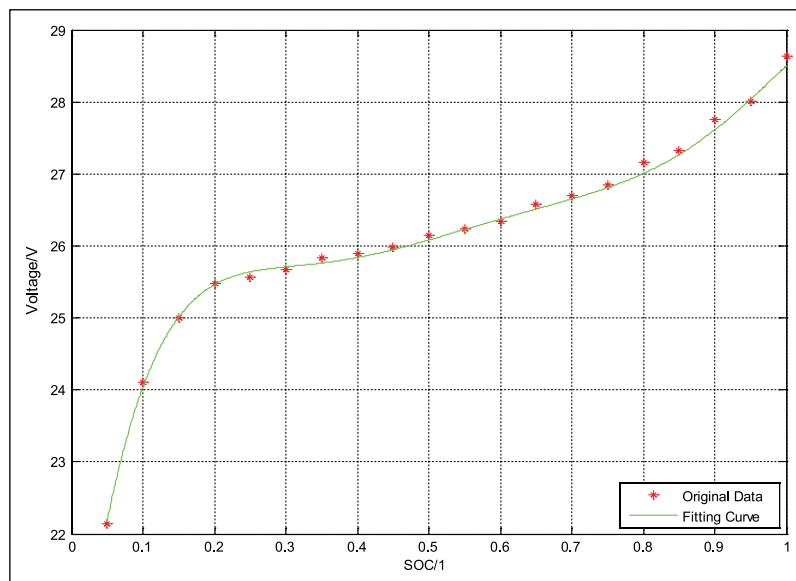


Figure 3. The relationship between OCV and SOC parameters.

battery packs are obtained by taking the charge and discharge difference effects into account, which are used in the parameter identification of the S-ECM model.

OCV parameter identification

The parameters of the S-ECM model can be identified and the evaluation value can be obtained by selecting the experimental samples of typical aerial lithium-ion battery packs, in which the OCV parameter U_{OC} is very important in the equivalent model. Aiming to measure its value accurately, the long no-use time is usually needed to make the working state of the battery down lag effect for removal of polarization phenomena and their introduction. The extraction of

this value can be achieved quickly through the charging and discharging process in the HPPC test, and the specific process is described as follows. The voltage will be increased slowly after the 40.00-s time lag effect under the polarization effect influence, at the end time point of which the voltage selected and used for the t_2 time moment. The lag effect under the influence of voltage will be reduced slowly after charging the 40 s on time, in which the voltage values at the end of the use of t_4 are selected. The charge and discharge time periods are very short and equal, so there is no change for the SOC value and the lag effect offset each other under the effect of the value. The OCV value through t_2 and t_4 time points can be gained, so the average value can be obtained by equation (4)

Table 2. The coefficient of relation between OCV and SOC.

Coefficient name	a_0	a_1	a_2	a_3	a_4	a_5	a_6
Numerical value	18.9	83.9	-417.7	1058	-1417	959.6	53.8

$$U_{OC} = \frac{(U_2 + U_4)}{2} \quad (4)$$

The relationship between the OCV and the SOC value can be obtained through the reduction process of the periodic SOC experiments. In addition, the dynamic simulation equations are obtained by fitting the experimental OCV–SOC results. The original and experimental SOC values can be estimated, respectively, on the mathematical description by using the percentage (%), in which the reasonable interval time results can be characterized. The simulation results and the dynamic OCV–SOC curve can be obtained as shown in Figure 3.

The curve change has obvious steep change zone, including the slowly change area and the steep change area. These three stages can be described by the subsection, so as to obtain the dynamic simulation and SOC estimation effect. The least square fitting curve of OCV–SOC that is based on the experimental data can be obtained and used for model parameter identification through the experiments and data analysis. The polynomial curve fitting method is used in the state equation expression in order to obtain the mathematical equation form and describe the relationship between OCV and SOC in the graph. The comparative analysis of fitting effect is conducted by the fitting equations shown in equation (5)

$$U_{OC} = f(\varphi) = a_0 + a_1\varphi + a_2\varphi^2 + a_3\varphi^3 + a_4\varphi^4 + a_5\varphi^5 + a_6\varphi^6 \quad (5)$$

The variable voltage is used to characterize the charge state SOC in the above expression, and the variable U_{OC} represents the OCV. The coefficients in the state space equations are obtained by fitting the experimental data curves in the graph. The coefficient values are shown in Table 2.

According to the experimental results, the fitting equation has perfect effect on the working characteristic simulation of the aerial lithium-ion battery packs. The relationship between the parameter OCV and the parameter SOC is used for the subsequent SOC estimation and the output voltage tracking of the aerial lithium-ion battery packs. According to the aerial safety monitoring demands at high pressure, the relationship curve between the OCV and the SOC for the aerial lithium-ion battery pack can be obtained corresponding to the feature of the SOC estimation section described by the above experiments. According to the state space equation of the established battery model, the parameters of $\varphi_0(X)$, $\varphi_1(X)$, ..., $\varphi_n(X)$ are assumed to be linear independent functions on the interval $C[a, b]$. The relationship can be expressed by means of $\varphi = \text{span}\{\varphi_0(X), \varphi_1(X), \dots, \varphi_n(X)\}$,

and then the function $S(x)$ can be calculated to minimize the sum value of the error squares. The procedure is shown in equation (6)

$$\begin{cases} \|\delta\|^2 = \sum_{k=0}^m \delta_i^2 = \sum_{k=0}^m [S(x(k)) - y(k)]^2 = \\ \min_{S(x)=\varphi} \sum_{k=0}^m [S(x(k)) - y(k)]^2 \\ S(x) = a_0\varphi_0(x) + a_1\varphi_1(x) + \dots + a_n\varphi_n(x) \end{cases} \quad (6)$$

Among them, the fitting curve of equation $S(x)$ can be obtained by the second part of the above equation, which can be also used for obtaining the function curve fitting equation based on the least squares method. The evaluation parameter (minimum mean square error (MMSE)) is used as the judgment basis in the model parameter identification process, and then the optimal estimation effect can be achieved in this way. According to the analysis of discharge process curve and equivalent model, the parameter identification of equivalent model is realized by using the partial least square algorithm. In addition, the model parameter identification result and its fitting effect are described as follows. The variance parameter (sum squared error (SSE)) value is 0.04983, which describes the discharge voltage data sequence square error and R^2 (regression-square) is the coefficient of determination, the fitted value of which is 0.9987. Meanwhile, the value of the error characterizing parameter (root mean square error (RMSE)) is found to be 0.06191. The OCV–SOC relationship can be described accurately based on the least square polynomial fitting.

Differential resistance calculation

The internal resistance value of the lithium-ion battery is ca. 1.00–20.00 m Ω , the value which determines the capacity of the battery. The value varies with the temperature and the working state of the battery in the application process. The influence of the internal resistance of the battery is often neglected in the research of the usual SOC estimation method. Thus, the error of the SOC estimation increased accordingly. The battery internal resistance tester AT520B is used in the experimental process, realizing the internal resistance determination under different SOC value for the aerial lithium-ion battery pack. The measuring range is 0.01 m Ω –300.00 Ω and the accuracy is 0.50%. The internal resistance test is obtained for the aerial lithium-ion battery pack through the experimental design process, where the test process is shown as follows. First, the battery is set to be full through the constant current to constant voltage charging process. Second, the aerial lithium-ion battery

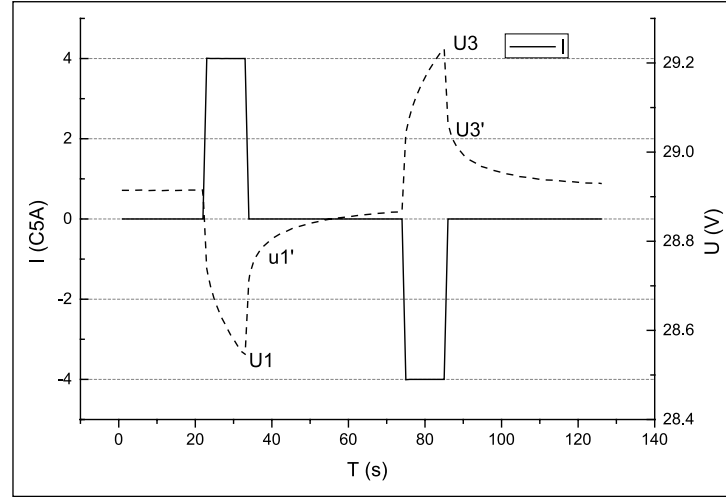


Figure 4. Variation of voltage and current in experimental HPPC test.

pack sample is discharged by using the 1C₅A discharging current on discharge for 6.00 min and the cyclic resistance can be measured after it is set aside for 1.00 h. The experimental test should be conducted until the SOC value changed from 100.00% to 0.00%. The internal resistance test results of the aerial lithium-ion battery pack can be obtained by measuring the internal resistance changes under different SOC conditions.

The experimental results show that the internal resistance varies in the discharging process, but the discharge will increase slightly in the later stage along with the continuous discharge process. As can be known from the experimental result analysis for the relationship of internal resistance and SOC, the internal resistance of the aerial lithium-ion battery pack remains at 0.48 mΩ. The fluctuation under different conditions is less than 0.02 mΩ. The internal resistance value is basically stable in the parameter identification process and subsequent SOC estimation in which it can be treated as a fixed value. In addition, the fluctuation is incorporated into the estimation process to make minor corrections.

There will be instantaneous rise and fall of the closed circuit voltage when the pulse discharge and charge of the aerial lithium-ion battery pack are stopped in the HPPC test process. The phenomenon can be characterized by the ohmic resistance R_{Ω} and the charge and discharge resistance difference of R_d and R_c . The charge and discharge resistance difference can be obtained by renovating the public ohm resistance R_{Ω} . The change of voltage and current in the experiment are shown in Figure 4.

Combined with the above analysis, the initial voltage at the pulse discharge stopping time point and the fast raised voltage can be set as U_1 and U_1' , respectively. Meanwhile, the initial voltage at the pulse charging stop time point and the rapidly decreased voltage can be set as U_3 and U_3' , respectively. The charge and discharge resistance difference can be described by using the parameters of R_d and R_c , respectively. The calculation process is shown in equation (7)

$$R_d = \frac{U_1 - U_1'}{I} - R_{\Omega}; \quad R_c = \frac{U_3 - U_3'}{I} - R_{\Omega} \quad (7)$$

The difference of charging and discharging resistance can be embedded in the SOC estimation process through the calculation and the ways of expression. This is used to characterize the aerial lithium-ion battery pack, improving the SOC estimation accuracy in the charging and discharging process.

Self-discharging resistance parameter acquisition

A series equalizing charging mode are adopted. In addition, the lithium-ion battery pack is charged to full capacity combined with a constant current fast charging mode to a constant voltage supplementary mode. The OCV $U_{OC}(1)$ is measured after 1.00 h and the OCV $U_{OC}(2)$ is measured after 30 days. After then, the SOC variation can be obtained by combining the OCV–SOC curve. As the OCV change is small, the average voltage of these two points can be taken as the self-discharge voltage in the discharge process. The self-discharge process is considered to be the constant current discharge by using the current I , combined with the relationship between rated capacity and power “1 Ah = 1 amp * 3600 s = 3600 ampere-second = 3600 Coulomb.” The relationship of the parameters of S-ECM model can be obtained as shown in equation (8)

$$\begin{cases} R_s = \frac{(U_{OC}(2) - U_{OC}(1))/2}{I} \\ I = \frac{\Delta Q}{\Delta t} = \frac{\{SOC(2) - SOC(1)\} Q_n * 3600}{\Delta t} \end{cases} \quad (8)$$

The self-discharge effect and the equivalent large resistance parameter R_s can be obtained through the joint analysis of the above expressions as shown in equation (9)

$$R_s = \frac{\{(U_{OC}(2) + U_{OC}(1))/2\} * \Delta t}{\{SOC(2) - SOC(1)\} * Q_n * 3600} \quad (9)$$

$$= \frac{\{(28.637 + 28.293)/2\} * 30 * 24 * 3600}{\{100.00\% - 97.37\% \} * 45 * 3600} = 1.73 * 10^4 \Omega$$

Then, the internal resistance factor K_s of the unit capacity for the single battery cell can be obtained. Furthermore, the correlation between the self-discharge resistance R_s and the battery cell number n together with the rated capacity Q_n can also be achieved. Finally, the determinant coefficient constant K_s of the discharge effect can be attained as shown in equation (10)

$$K_s = \frac{\Delta SOC}{\Delta t} = \frac{\{SOC(2) - SOC(1)\}}{\Delta t} \quad (10)$$

$$= \frac{100.00\% - 97.37\%}{30 * 24 * 3600} = 1.0147 * 10^{-8}$$

When the aerial lithium-ion battery pack is in charge and discharge state, the direction of discharge current is assumed to be the positive direction. The function relation in the SOC iterative calculation is described as the mathematical expression of the state equation in the SOC estimation process according to the S-ECM model. Considering the self-discharge internal resistance (R_s) influence, the state equation of the continuous state space equation is constructed as shown in equation (11)

$$SOC(t) = SOC(0) - \int_0^t \frac{\eta_l \eta_T I(\tau)}{Q_n} d\tau - \int_0^t \frac{I_s(\tau)}{Q_n} d\tau \quad (11)$$

wherein, $SOC(t)$ represents the SOC value at t time moment, and $SOC(0)$ is the SOC value at the initial time point. η_l represents the coulombic efficiency under different current I . η_T denotes the temperature effects on the coulombic efficiency. Q_n is the rated capacity of the battery pack. $I_s(t)$ is the self-discharge current and the resistance R_s is used to characterize the self-discharge effect of the aerial lithium-ion battery pack, the expression of which is shown in equation (12)

$$I_s(t) = \frac{U_{OC}(t)}{R_s} \quad (12)$$

By using the state space model in the charge and discharge process combined with the identification process of the model parameters, the basic equation framework of the estimation process is established for subsequent SOC estimation research. On the basis of determining the state space equation, the design of model parameter identification system is carried out. According to the requirements in the estimation process, the equivalent model and state space equation of the aerial lithium-ion battery pack are established. Bestowing to the parameters of closed circuit

voltage, voltage, current and temperature of the battery pack, the system state equation is constructed through the model parameter identification. As the data acquisition and processing are discrete time forms in the actual calculation process, the iterative calculation process of the state equation is shown in equation (13)

$$SOC(k | k-1) = SOC(k-1) - \frac{\eta_l \eta_T I(k) T_s}{Q_n} - K_s * T_s \quad (13)$$

The parameters used in the above equation can be described as follows. k is the time point of the SOC estimation for the aerial lithium-ion battery pack. $U_L(k)$ is the closed circuit voltage of the battery pack at the k time point. R_o signifies the Ohm internal resistance of the aerial lithium-ion battery pack. $I(k)$ is the output current of the battery pack. K_s is the SOC change amount of the battery pack in each detection cycle. T_s is the parameter detection cycle period of the battery pack, that is, the signal sampling time interval. Afterward, the estimated SOC value can be corrected in the working process by taking the self-discharging effect into the state equation of the aerial lithium-ion battery pack.

RC parallel parameter acquisition

When the aerial lithium-ion battery pack is in the HPPC discharging process, the voltage will have a slow process after the rapid process because of the influence of the polarization effect. There is half an hour abeyance before the pulse discharge, so the influence of the polarization effect is becoming very small. The working state of the polarization RC parallel circuit can be recognized as the zero state response in the 10-s pulse discharging process. Thus, the polarization resistance R_p can be obtained and the calculation process can be described as shown in equation (14)

$$\begin{cases} U_L = U_{OC} - IR_{\Omega} - U_p - IR_d \\ U_p = IR_p (1 - e^{-t/\tau}) \end{cases} \quad (14)$$

The parameters of OCV U_{OC} , Ohm inside resistance R_{Ω} and discharging difference inside resistance R_d in the above equation can be obtained by the frontal calculation process, and the polarization resistance R_p in the discharging process can be calculated. The polarization inside resistance R_p can be achieved by using a similar method. As there is only 40s shelved time before the multiple charging maintenance, the influence of the polarization effect cannot be eliminated completely. As a result, the RC parallel circuit response in the pulse charging process can be recognized as the common effect of the zero input response and the zero state response. Thus, the polarized resistance at this time point can be calculated as shown in equation (15)

$$\begin{cases} U_L = U_{OC} - IR_{\Omega} - U_p - IR_d \\ U_p = U_p(0)e^{-t/\tau} + IR_p (1 - e^{-t/\tau}) \end{cases} \quad (15)$$

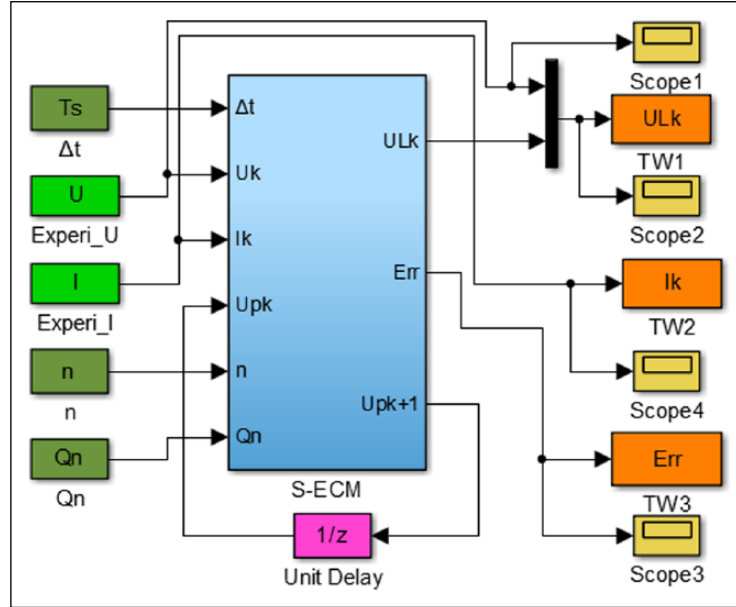


Figure 5. The experimental effect test structure of the S-ECM model.

The parameters of OCV U_{OC} , Ohm inside resistance R_{Ω} and discharging difference inside resistance R_d in the above equation can be obtained in the experimental pulse test analysis. Just for the convenient calculation, the zero input response of the RC parallel circuit can be equivalent to the extender of the zero input response when the pulse discharging becomes into the shelved state. As a result, the voltage on the polarized capacity C_p at the ending time point of the pulse discharge can be used as the parameter value of $U_p(0)$, and the polarized inside resistance R_p can be calculated and obtained. The calculation equation can be achieved according to the relationship of the polarization resistance R_p , polarization capacity C_p and the time constant τ in the calculation process. The inference process is shown in equation (16)

$$\tau = R_p C_p \Rightarrow C_p = \frac{\tau}{R_p} \quad (16)$$

The variation of the model parameters can be attained and embedded into the state space equation for the subsequent SOC estimation by the curve fitting for the S-ECM model and the analogy circuit voltage relationship expression between U_{OC} and SOC in the acquisition process.

Experimental analysis

Modular design of parameter identification process

After identifying the parameters of the targeted S-ECM model, the dynamic simulation model is built according to the dynamic modeling analysis of the system. The experiment is carried out to verify the tracking effect of the output voltage based on the constructed S-ECM model. There are differences in the aerial lithium-ion battery pack among the

connected battery cells due to the production and the aging process. As a result, the experimental parameter identification process is limited by a single maximum or minimum battery voltage, temperature and current rate of the battery cells. In the experimental process, these parameters will be monitored in real-time, and the corresponding stop operation should be carried out by the threshold judgment. Once the experiment is stopped by the above conditions, the experiment under this temperature and current rate condition has ended and the obtained values are used as experimental data for further analysis.

In the energy flow controlling and optimizing process of the power source and the electrical load, the available energy of an aerial lithium-ion battery is defined as an additional state in the estimation process. Furthermore, the system state space equation can be rewritten and used for the adjustable parameter identification of the SOC estimation process. The total voltage, cell voltage, charge/discharge current and temperature are detected in real time in order to avoid sudden voltage drop and current pulse. In addition, it can also be applied effectively to the state estimation of the aircraft lithium-ion battery. Among them, the model structure of the identification system plays a key role in the estimation process, especially in the rewriting result of parameter calculation process and the initialization characterization of the parameter vector. The S-ECM equivalent circuit model is set up by using the above calculation process, which is shown in Figure 5.

The symbols in Figure 5 are described as follows: the input parameters of Ts model in S-ECM for parameter detection cycle, and the model calculation of the OCV, current and SOC parameters in the experimental process, the output voltage of ULk as well as the tracking error value Err. In view of the discrete time calculation process of the model parameters, the model is designed to calculate the structure of the sub-module S-ECM, as shown in Figure 6.

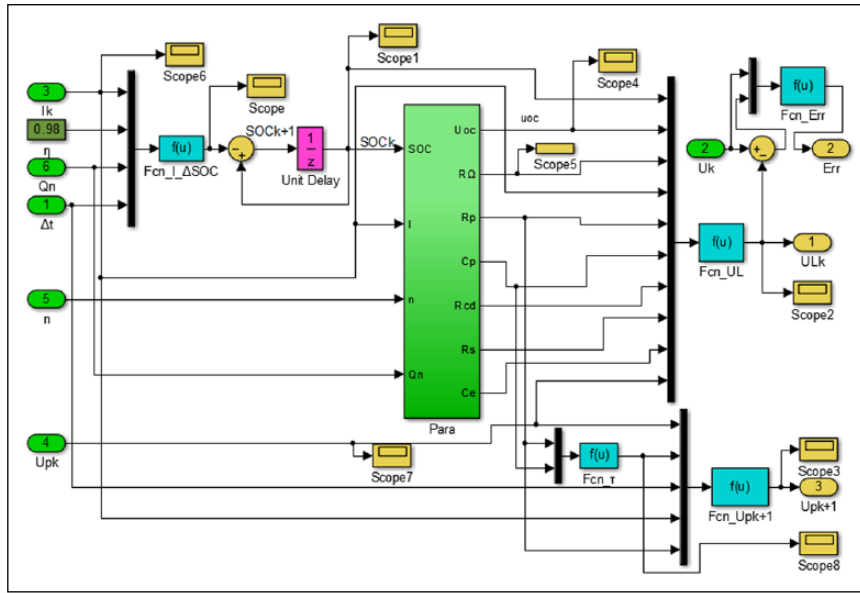


Figure 6. The model calculation sub-module.

Each step in the calculation process is shown as follows. (1) During the test, the voltage of Experi_U and Experi_I parameter are employed to obtain the current discharge process through the discharge experiment method. In addition, the sampling interval parameters of ΔT is used for subsequent output voltage calculation model based on the tracking effect analysis. (2) According to the discrete current, the detected $I(k)$ is combined with the sampling interval of ΔT for the calculation process based on current time integral function Fcn_I. Next, u is constructed into $\Delta SOC = (2) \times u(4) / (U(3) \times 3600) \times u(1)$, change the SOC parameter calculation into the discharge process. (3) Using OCV, the identification results were calculated. In addition, the OCV U_{OC} , the ohmic resistance, structure polarization resistance and the polarization capacitance were calculated using the model parameter calculation module of Para. (4) Furthermore, the polarization resistance and polarization capacitance were calculated according to the product parameters of RC parallel circuit time constant. The time constant calculation function was employed to construct the polarization of RC parallel circuit voltage. The calculation process was determined by using the following mathematical expression: $Fcn_Upk+1 = U(1) \times \exp(-u(3)/u(2)) + u(4) \times u(5) \times (1 - \exp(-u(3)/u(2)))$ according to formula (5). Afterward, it is used to construct the output voltage tracking calculation function of $Fcn_UL = u(2) - u(3) \times u(4) - u(10) - u(4) \times u(7)$. The Para module output along with polarization voltage parameter Upk and ULk was utilized for the calculation process. Therefore, the values were compared to the value of the battery and the detected voltage.

As can be deduced from the experimental analysis, the model has respectable tracking effect on the output voltage, which reflects the changing law of the voltage. The identification designed model of the self-learning property shows that the identification method is also considering the aging situation. The current state is determined by the prediction

of energy supply to meet the demand of power. In the process of parameter identification of the group S-ECM model, a test experiment was carried out in advance to establish the relationship between SOC and voltage as well as current and temperature parameters of the aerial lithium-ion battery pack. The model identification process can be obtained by constructing the model and its output as the identification result. It is very difficult to achieve the OCV value online, as it cannot be attained directly during charging-discharging process. Therefore, it is obtained by using the feedback calculation of the SOC parameter values.

Experimental results of parameter identification results

T_a is set as the discharge time for the instrument check treatment. T_b is employed to indicate discharge time of the airplane ignition. T_c indicates the supplementary electric time. T_d simulates the self-discharge time and T_e is the emergency output time of the lithium-ion battery pack. The experimental steps are described as follows. S1: Determine whether the single cell voltage and the total voltage of the battery pack are greater than the minimum voltage 3 and 21 V. Enter the second step if it is meeting the conditions otherwise move to the 10th step. S2: Stay for 10 s and turn to the third step. S3: Discharge using 0.3C for T_a seconds to simulate the instrument check process and determine whether the battery cell voltage and total voltage are greater than the minimum voltage at the same time. If the values meet the conditions, it should enter the fourth step, otherwise move to the 10th step. S4: Simulate the aircraft ignition with 0.6C discharge for T_b seconds and judge whether the monomer voltage and the total voltage are greater than the minimum voltage. If the values meet the conditions, it should enter the fifth step, otherwise move to the 10th step. S5: Charge the battery pack by using the 0.1C current rate for T_c seconds to simulate the

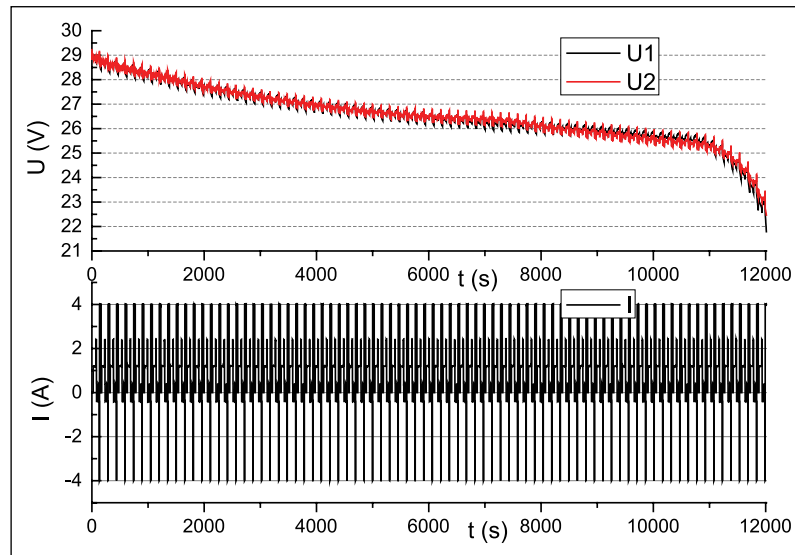


Figure 7. The fitting results in the S-ECM parameter identification process.

replenish electricity process and turn to the sixth step. S6: Simulate the self-discharge of the lithium-ion battery pack with a 0.01C discharge of Td seconds, and then enter the seventh step. S7: Charge the battery pack by using the 0.1C current rate for Tc seconds to simulate the replenish electricity process and turn to the eighth step. S8: The battery pack should be discharged with 1C current rate for Te seconds to simulate the emergency output. The phenomenon should be judged whether the cell voltage and the total voltage are greater than the minimum voltage. The process turns to the ninth step when meeting the requirements. Otherwise, it should move to the 10th step. S9: The experiment will jump to step 10 if the cell voltage reaches 3V or the pack voltage reaches 21V. Otherwise, the experiment will jump to the step 2. S10: The process ends.

The variable voltage and current parameters can be obtained in the state estimation method according to the data achieved in the experimental process. Afterward, the output voltage of the tracking results can be obtained by considering the rated capacity and the cell number of the aerial lithium-ion battery pack. Meanwhile, the terminal voltage can be estimated by updating the estimation process constantly. The time parameters are initiated as follows: $Ta(60s)$, $Tb(5s)$, $Tc(20s)$, $Td(10s)$, $Te(50s)$. The actual current I is detected by using the electronic load in the model calculation process. Considering the influence of temperature and resistance, the discharge efficiency is set as 0.98. The sampling interval is 1.00s and the charge and discharge current values are obtained by using the real-time detection process. After the voltage comparison of the detected and estimated values are realized, the output voltage of the fitting and tracking results is obtained as shown in Figure 7.

The experimental results show that the battery equivalent design model can reflect the state changes of the aerial lithium-ion battery pack. The S-ECM is used for the battery modeling to construct the equivalent model. As the experimental analysis shows, the experimental results have been obtained. The realization of the output voltage tracking

treatment solves better the working state monitoring problem. The proposed equivalent model can well characterize the reaction process of the aerial lithium-ion battery pack well. The method is implemented by using the circuit equivalence, and experimental results are obtained, which can solve the SOC estimation problem of the aerial lithium-ion battery pack effectively. During the charging process, the constant current discharge is conducted by setting the simulated current. It turns to the constant current supplementary power when the voltage reaches the end voltage and is calculated according to the actual current value of the detected numerical control power supply. The voltage comparison of detected value is realized toward the calculated value. Thus, the output voltage of the fitting tracking results can be obtained as shown in Figure 8.

As can be seen from the charge/discharge results of the experimental analysis, the tests have similar change rules. The voltage characteristics of the lithium-ion batteries are analyzed respectively, and the working characteristics are then obtained. As can be known from the above theoretical and experimental analysis, the estimation results under the charge/discharge conditions can be constructed by the S-ECM model and the measured value of the voltage variation. The tracking error is less than 2.00% and the model parameter identification results can well fit into the air lithium-ion battery performance.

Conclusion

The working characteristics of the lithium-ion batteries in groups are obtained through the experimental study of the working characteristics of the batteries. Based on the model equivalent analysis and characterization of the battery characteristics, the equivalent model S-ECM of the aerial lithium-ion batteries is determined. Therefore, the identification and determination model parameters are carried out. According to the experimental analysis of the tracking effect of the output voltage, the parameter identification

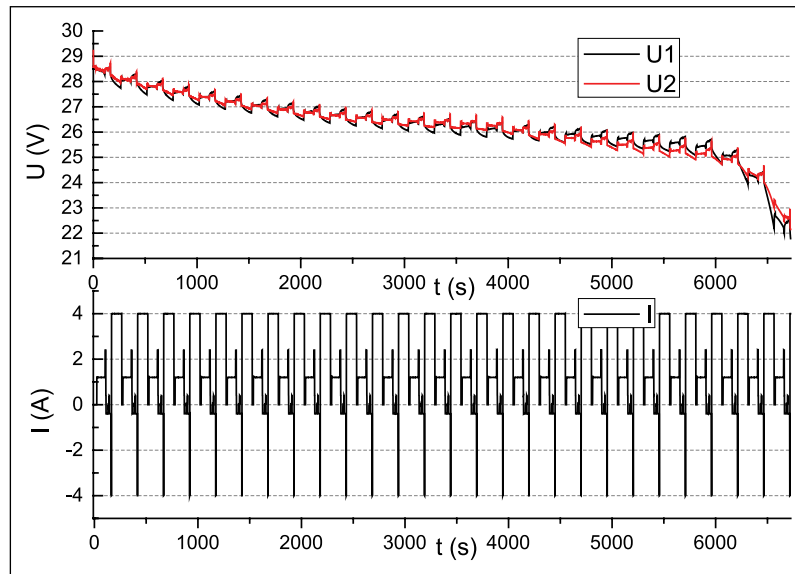


Figure 8. The fitting results in the S-ECM parameter identification process.

results of the proposed equivalent model have been verified. The experimental results show that the model can be used to characterize the work characteristics during the charging and discharging process. Therefore, the model can be used for the accurate estimation of SOC. Furthermore, the S-ECM equivalent model and state space equation are finally determined by analyzing the voltage characteristics of the aerial lithium-ion battery pack.


Acknowledgements

C.F. would like to express his gratitude to RGU for support. The authors would like to express their gratitude to the sponsors.

Funding

The work was supported by The National Defense Scientific Research (No. B3120133002), Sichuan Science and Technology Support Program (No. 2017FZ0013), Scientific Research Fund of Sichuan (No. 17ZB0453) and Sichuan Science and Technology Innovation Cultivation Project (No. 201710619112). Furthermore, the early work was supported by Mianyang Science and Technology Project (No. 15G-03-3) and Innovative Training Program in Sichuan (No. 201410619004).

ORCID iD

Shunli Wang  <https://orcid.org/0000-0003-0485-8082>

References

1. Beattie SD, Loveridge MJ, Lain MJ, et al. Understanding capacity fade in silicon based electrodes for lithium-ion batteries using three electrode cells and upper cut-off voltage studies. *J Power Sources* 2016; 302: 426–430.
2. Bauer M, Wachtler M, Stowe H, et al. Understanding the dilation and dilation relaxation behavior of graphite-based lithium-ion cells. *J Power Sources* 2016; 317: 93–102.
3. Wang SL, Fernandez C, Shang LP, et al. An integrated online adaptive state of charge estimation approach of high-power lithium-ion battery packs. *T I Meas Control* 2018; 40(6): 1892–1910.
4. Cacciato M, Nobile G, Scarcella G, et al. Real-time model-based estimation of SOC and SOH for energy storage systems. *IEEE T Power Electr* 2017; 32(1): 794–803.
5. Chen WC, Wang YW and Shu CM. Adiabatic calorimetry test of the reaction kinetics and self-heating model for 18650 Li-ion cells in various states of charge. *J Power Sources* 2016; 318: 200–209.
6. Chen XP, Shen WX, Dai MX, et al. Robust adaptive sliding-mode observer using RBF neural network for lithium-ion battery state of charge estimation in electric vehicles. *IEEE T Veh Technol* 2016; 65(4): 1936–1947.
7. Bresciana F, Rabissia C, Zagoa M, et al. A combined in-situ and post-mortem investigation on local permanent degradation in a direct methanol fuel cell. *J Power Sources* 2016; 306: 49–61.
8. Abadaa S, Marlairb G, Lecocqb A, et al. Safety focused modeling of lithium-ion batteries: A review. *J Power Sources* 2016; 306: 178–192.
9. Barai A, Uddin K, Widanalage WD, et al. The effect of average cycling current on total energy of lithium-ion batteries for electric vehicles. *J Power Sources* 2016; 303: 81–85.
10. Dubarry M, Devie A and Liaw BY. Cell-balancing currents in parallel strings of a battery system. *J Power Sources* 2016; 321: 36–46.
11. Hu XS, Zou CF, Zhang CP, et al. Technological developments in batteries: A survey of principal roles, types, and management needs sign in or purchase. *IEEE Power Energy M* 2017; 15(5): 20–31.
12. Jiang JC, Ruan HJ, Sun BX, et al. A reduced low-temperature electro-thermal coupled model for lithium-ion batteries. *Appl Energ* 2016; 177: 804–816.
13. Koca YB, Oguz Y, Yonetken A, et al. Investigation efficiency and microcontroller-based energy flow control for wind-solar-fuel cell hybrid energy generation system with battery storage. *Meas Control* 2016; 50(7): 159–168.
14. Li XY, Fan GD, Rizzoni G, et al. A simplified multi-particle model for lithium ion batteries via a predictor-corrector strategy and quasi-linearization. *Energy* 2016; 116: 154–169.
15. Lim K, Bastawrous HA, Duong VH, et al. Fading Kalman filter-based real-time state of charge estimation in LiFePO4

- battery-powered electric vehicles. *Appl Energ* 2016; 169: 40–48.
16. Liu CZ, Liu WQ, Wang LY, et al. A new method of modeling and state of charge estimation of the battery. *J Power Sources* 2016; 320: 1–12.
 17. Liu T, Zou Y, Liu DX, et al. Energy management for battery electric vehicle with automated mechanical transmission. *Int J Vehicle Des* 2016; 70(1): 98–112.
 18. Martel F, Dube Y, Kelouwani S, et al. Long-term assessment of economic plug-in hybrid electric vehicle battery lifetime degradation management through near optimal fuel cell load sharing. *J Power Sources* 2016; 318: 270–282.
 19. Ozer T, Oguz Y, Cimen H, et al. Energy flow control with using Arduino microcontroller in off-grid hybrid power generation system including different solar panels and fuel cell. *Meas Control* 2017; 50(9): 186–198.
 20. Sarasketa-Zabala E, Martinez-Laserna E, Berecibar M, et al. Realistic lifetime prediction approach for Li-ion batteries. *Appl Energ* 2016; 162: 839–852.
 21. Saw LH, Ye YH, Tay AAO, et al. Integration issues of lithium ion battery into electric vehicles battery pack. *J Clean Prod* 2016; 113: 1032–1045.
 22. Soylu E and Bayir R. Measurement of electrical conditions of rechargeable batteries. *Meas Control* 2016; 49(2): 72–81.
 23. Sung W, Hwang DS, Nam J, et al. Robust and efficient capacity estimation using data-driven metamodel applicable to battery management system of electric vehicles. *J Electrochem Soc* 2016; 163(6): A981–A991.
 24. Sung W, Hwang DS, Jeong BJ, et al. Electrochemical battery model and its parameter estimator for use in a battery management system of plug-in hybrid electric vehicles. *Int J Auto Tech* 2016; 17(3): 493–508.
 25. Wang SL, Shang LP, Li ZF, et al. Online dynamic equalization adjustment of high-power lithium ion battery packs based on the state of balance estimation. *Appl Energ* 2016; 166: 44–58.
 26. Wang SL, Fernandez C, Chen MJ, et al. A novel safety anticipation estimation method for the aerial lithium-ion battery pack based on the real-time detection and filtering. *J Clean Prod* 2018; 185: 187–197.
 27. Wang YJ, Zhang CB, Chen ZH, et al. An adaptive remaining energy prediction approach for lithium-ion batteries in electric vehicles. *J Power Sources* 2016; 305: 80–88.
 28. Wei ZB, Meng SJ, Xiong BY, et al. Enhanced online model identification and state of charge estimation for lithium ion battery with a FBCRLS based observer. *Appl Energ* 2016; 181: 332–341.
 29. Zhou DM, Zhang K, Ravey A, et al. Parameter sensitivity analysis for fractional-order modeling of lithium-ion batteries. *Energies* 2016; 9(3): 123.
 30. Zou HM, Wang W, Zhang GY, et al. Experimental investigation on an integrated thermal management system with heat pipe heat exchanger for electric vehicle. *Energ Convers Manage* 2016; 118: 88–95.